Analysis of the Impact of Earthquakes on the Stability of Overlying Fill Slopes

Bin li and Wensheng Hou

Abstract Earthquakes are one of the main factors causing landslides. In this paper, the author conducted a numerical simulation of an overlying fill slope in Guangxi, the subject, with Midas GTS under the vibration conditions of magnitude 6, 6.5, 7, 7.5, and 8 earthquakes and obtained the total, horizontal and vertical displacement of the slope and its stability coefficient. The results showed that the displacement of the slope increased with the increase of the seismic acceleration; its maximum displacement occurred in the middle of the slope (fill); the difference of the maximum horizontal displacement from the total displacement and vertical displacement was that as the seismic acceleration increased, the maximum horizontal displacement occurred not only in the middle of the slope (fill), but also at the top and on the middle and upper surfaces; the vertical displacement was most susceptible, while the horizontal displacement was least susceptible; as the magnitude increased, the stability coefficient of the slope also decreased significantly; and, vegetation planting on the slope and the setup of a retaining wall at the foot could improve its stability coefficient effectively. Therefore, it was necessary to plant vegetation on a slope and set up a retaining wall at the foot.

Keywords Earthquakes · Stability analysis · Slope · Midas GTS · Numerical simulation

B. li (✉)
Tianjin Port Engineering Institute Co., Ltd. of CCCC First Harbor Engineering Co., Ltd., Tianjin 300222, China
e-mail: lee_binbin@163.com

Key Laboratory of Port Geotechnical Engineering, Ministry of Communications, PRC, Tianjin 300222, China

Key Laboratory of Tianjin Port Geotechnical Engineering, Tianjin 300222, China

CCCC First Harbor Engineering Company Ltd., Tianjin, China

W. Hou
Jiangsu Weihua Ocean Heavy Industry Co., Ltd., Changyuan County, China

Y. Yang (ed.), *Advances in Frontier Research on Engineering Structures*, Lecture Notes in Civil Engineering 286, https://doi.org/10.1007/978-981-19-8657-4_41

1 Introduction

China has a vast territory, a large proportion of which is taken up by mountainous areas. Natural slopes are widely distributed throughout the country. Many artificial slopes have been built to ensure the safety of railways and highways during their construction and use. China located in an earthquake-prone area is characterized by frequent earthquakes, high magnitude, and wide distribution [1]. Almost all magnitude 8 earthquakes and 80–90% of strong earthquakes of magnitude 7 and above in mainland China occurred in the boundary zone of active tectonic blocks, indicating that China is a country with frequent earthquakes [2]. Slope instability (collapses and landslides, etc.) induced by earthquakes is often the main factor causing casualties and property losses in earthquakes [3]. The total number of landslides collapses and debris flows triggered by the 2008 Wenchuan earthquake was up to 30,000–50,000, including more than 12,600 sites with hidden hazards that directly threatened the safety and temporary resettlement of people after the earthquake (according to the statistics of 39 worst hit counties in Sichuan Province), of which there were dozens of giant landslides with a scale over 1000 $\times$ 104 m^3 [4]. The 2010 earthquake in Port-au-Prince, Haiti triggered about 30,000 landslides [5]. The disasters caused by slope instability are shocking. The analysis of the seismic stability of slopes has become one of the important topics in geotechnical engineering and seismic engineering fields [6]. In China, studies on the dynamic stability of slopes were mostly conducted based on the dynamic stability coefficient. The research methods can be roughly divided into the quasi-static method [7], dynamic time-history method [8] and dynamic strength reduction method [9]. In this paper, the slope was simulated with the finite element method through modeling with Midas-GTS to study the law and characteristics of the stability of the overlying fill slope under seismic conditions.

2 Determination of Model Dimensions and Parameters

2.1 Slope Dimensions

The subject, an overlying fill slope in Guangxi, was covered with vegetation on the surface and provided with a retaining wall at the foot. Figure 1 shows the geometric dimensions of the slope. Mechanical parameters of slope rocks and soil masses.

Mechanical parameters of slope rocks and soil masses are shown in Table 1. The slope surface was covered with vegetation and the plant roots could greatly improve the shear strength of soils [10]. With the increase of the root length density and surface area density, the internal friction angle (φ) of soil increased logarithmically and its cohesion (c) increased linearly and significantly [11]. Therefore, the internal friction angle and cohesion of soil on the slope surface were increased appropriately in this paper.

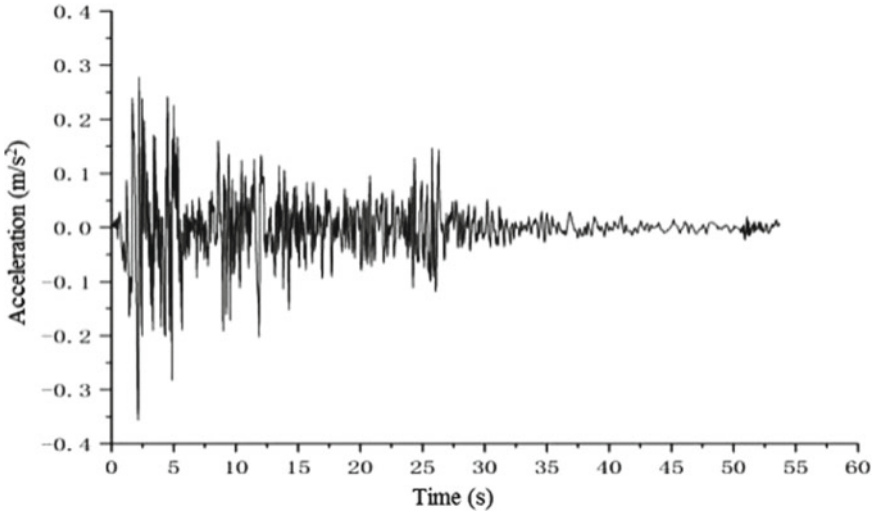

Fig. 1 Seismic acceleration time history

Table 1 Basic parameters of slope rocks and soil masses

Soil layer	Soil mass	Unit weight γ (KN/m^3)	Internal friction angle φ(°)	Cohesion c (MPa)	Initial void ratio e	Poisson's ratio v	Elastic modulus E (GPa)
Soil layer 1	Moderately weathered slate	24	55	85	0.5	0.25	25
Soil layer 2	Strongly weathered slate	22	28	66	1	0.2	16
Soil layer 3	Silty clay	18.5	15	30	1	0.3	0.03
Topsoil	Root soil	18.5	25	36	1	0.3	0.03

2.2 Boundary Conditions

Dynamic wave reflection would exist on the boundary during dynamic calculation, which would affect the dynamic calculation results to some extent. Therefore, Midas-GTS provided two boundaries in the dynamic calculation, namely static boundary, and free field boundary. Input wave reflection at the boundary of the model could be reduced through the designation of different boundary conditions. The free field boundary was selected as the boundary condition in the dynamic calculation based on the actual conditions of the model slope. Due to the large modulus of the model material, the input wave could be applied directly to the bottom of the model as an

acceleration time-history curve or velocity time-history curve, and it was unnecessary to apply a static boundary to the bottom [12].

3 Design of Seismic Conditions

The slope stability under the conditions of magnitude 6, 6.5, 7, 7.5, and 8 earthquakes was studied. Peak acceleration is 0.05, 0.075, 0.1, 0.15, and 0.2 g according to the Code for Seismic Design of Buildings [13].

The acceleration time-history curve is shown in Fig. 1:

4 Analysis of Slope Stability Under Seismic Conditions

4.1 Displacement

(1) Total displacement

The total displacement of the slope under the conditions of seismic acceleration of 0.05, 0.075, 0.1, 0.15, and 0.2 g were get from computing.

A line chart of the maximum total displacement under the conditions of different seismic acceleration was drawn based on the total displacement diagrams under the five different conditions above, as shown in Fig. 2.

According to the analysis from the perspective of total displacement, the maximum total displacement under the five different conditions was 0.023 m, 0.035 m, 0.407 m,

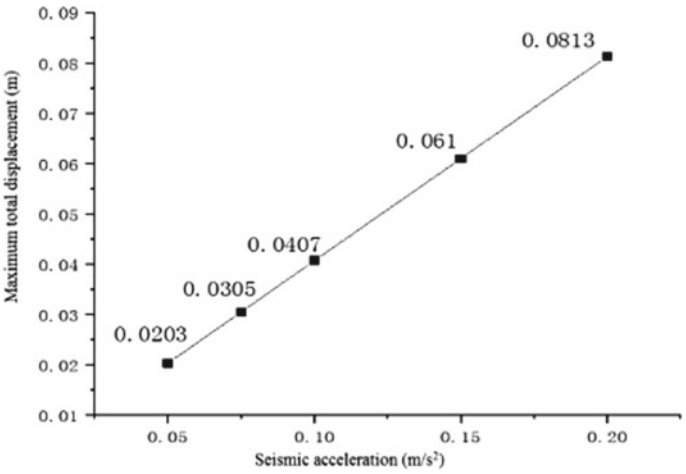

Fig. 2 Maximum displacement

0.061 m, and 0.081 m, respectively. The maximum displacement mainly occurred at the soil layer 3 (fill) because the shear strength of the slope was less than the total stress on it under the combined action of seismic stress and the gravity stress of the slope due to the low strength and stability of the soil layer 3 (fill). The corresponding displacement also increased with the increase of seismic acceleration. However, the total displacement at the slope bottom was almost zero because the retaining wall offset the landslide thrust of soil through the friction resistance generated by its gravity which improved its anti-sliding and anti-overturning abilities.

(2) horizontal displacement

The horizontal displacement of the slope under the conditions of seismic acceleration of 0.05, 0.075, 0.1, 0.15, and 0.2 g were get from computing. A line chart of the maximum horizontal displacement under the conditions of different seismic acceleration was drawn based on the horizontal displacement diagrams under the five different conditions above, as shown in Fig. 3.

The horizontal displacement was the smallest, which was 0.0040 m, 0.0061 m, 0.0399 m, 0.0599 m, and 0.0799 m under the five different conditions of 0.05 g, 0.075 g, 0.15 g, 0.1 g, and 0.2 g, respectively. The maximum displacement occurred at the top and on the middle and upper surfaces of the slope. What differs from the total displacement and vertical displacement was that the maximum displacement in the horizontal direction occurred not only at the soil layer 3 (fill), but also at the top and on the middle and upper surfaces of the slope, while there was hardly any displacement at the bottom of the slope.

(3) Vertical displacement

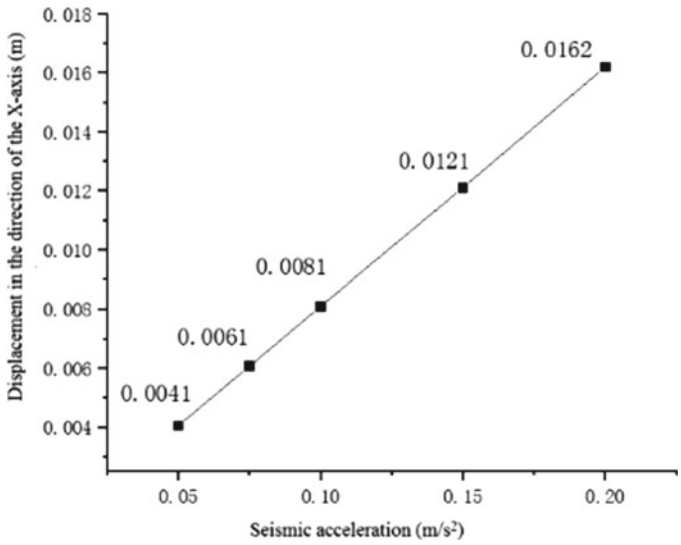

Fig. 3 Horizontal displacement

The vertical displacement of the slope under five conditions was get from computing. A line chart of the maximum vertical displacement under the conditions of different seismic acceleration was drawn.

The vertical displacement was relatively large, which was 0.0200 m, 0.0300 m, 0.0399 m, 0.0599 m, and 0.0799 m under the five different conditions of 0.05 g, 0.075 g, 0.1 g, 0.15 g, and 0.2 g, respectively. In general, the displacement mainly occurred at the soil layer 3 (fill) and decreased gradually from the middle to the foot and top of the slope.

It can be seen from the nephograms and line charts of the horizontal, vertical, and total displacement distribution under five different conditions that the maximum displacement mainly occurred at soil layer 3 (fill) for the reason that the shear strength of the slope was less than the total stress on it under the conditions of different seismic acceleration under the combined action of seismic stress and the gravity stress of the slope due to the low strength and stability of the soil layer 3 (fill), resulting in plastic fracture at different levels; however, the total displacement at the slope bottom was almost zero for the reason that the retaining wall offset the landslide thrust of soil through the friction resistance generated by its gravity which improved its anti-sliding and anti-overturning abilities.

4.2 Stability Coefficient

An analysis was conducted on the stability coefficient under the conditions of seismic acceleration of 0.05, 0.075, 0.1, 0.15, and 0.2 g and four different conditions (no vegetation or retaining wall; vegetation planting but no retaining wall; retaining wall setup but no vegetation; both vegetation planting and retaining wall setup) to analyze the stability of the slope with different reinforcement methods under different seismic acceleration conditions.

According to the results, the stability coefficient of the slope was 1.135, 1.117, 1.096, 1.048, and 0.986 respectively under the conditions of seismic acceleration 0.05, 0.075, 0.1, 0.15, and 0.2 g and different reinforcement measures. The energy released by an earthquake and its dynamic load increased geometrically with the increase of earthquake magnitude and acceleration, so the slope stability coefficient decreased greatly. The stability coefficient was only 0.986 under the condition of seismic acceleration of 0.2 g, in which case the slope became unstable and damaged. This shows the importance of the aseismic design of a slope. According to Table 3, the setup of a retaining wall at the foot of the slope could improve its stability coefficient. The stability coefficient of the slope was greatly improved under the condition of vegetation planting. Deep and thick roots had an anchoring effect, and shallow and thin roots had a reinforcing effect [14], which could improve the shear strength of soil masses [10] and thus the stability of the slope.

According to the comprehensive analysis above, the greatest damage to the slope occurred almost all in its middle part, indicating that the middle part was prone to

deformation and damage. Therefore, it was quite necessary to reinforce the slope by vegetation planting on the surface and setting up a retaining wall at the foot.

5 Conclusions

This paper mainly studied the impact of five different earthquake magnitudes (different earthquake acceleration) on slope stability and discussed the stability of the slope under seismic conditions from the perspectives of slope displacement and stability coefficient. The following conclusions were drawn:

1. Seen from the displacement nephograms, the maximum displacement occurred at soil layer 3 (fill). The corresponding displacement increased with the increase of the seismic acceleration. What differs from the total displacement and vertical displacement was that the maximum displacement in the horizontal direction occurred not only at the soil layer 3 (fill), but also at the top and on the middle and upper surfaces of the slope. According to the analysis of displacement susceptibility in each direction, the vertical displacement was the largest while the horizontal displacement was the smallest.
2. The slope stability coefficient decreased significantly with the increase of the earthquake magnitude. Planting vegetation on the slope and setting up a retaining wall at the foot could improve the stability coefficient of the slope effectively. Therefore, it was quite necessary to plant vegetation and set up a retaining wall for slopes with a low stability coefficient.

References

1. Zhang XD, Wang YY, He XJ (2022) Seismic hazards and earthquake prevention and mitigation. China Insur 02:35–39
2. Zhang PZ, Deng QD, Zhang GM, Ma J, Gan WJ, Min W, Mao FY, Wang Q (2003) Strong earthquakes and active blocks in mainland China. Sci China (Ser D: Earth Sci) S1:12–20
3. Keefer DK (1984) Landslides caused by earthquakes. Geol Soc Am Bull 95(4):406–421
4. Huang RQ (2009) Mechanism of landslide disasters triggered by Wenchuan M8.0 earthquake and its geomechanical model. Chin J Rock Mech Eng 28(06):1239–1249
5. Hough SE, Altidor JR, Anglade D et al (2010) Localized damage caused by topographic amplification during the 2010 M7.0 Haiti earthquake. Nat Geoence 3(11):778–782
6. Li HB, Jiang HJ, Zhao J, Huang LX, Li JR (2003) Several problems of rock mass engineering safety under dynamic load. Chin J Rock Mechan Eng 11:1887–1891
7. Li N, Cheng GD, Xie DY (2001) Rock mechanics problems in China's western development. Chin J Geotech Eng 03:268–272
8. Liu X, Tang HM, Hu XL, Wang LQ, Liao SB, Zou ZX (2012) Formation mechanism and dynamic stability of long-distance landslide on Jingu expressway. Chin J Rock Mechan Eng 31(12):2527–2537
9. Dai ML, Li TC (2007) Safety evaluation and analysis of dynamic stability of complex rock slopes based on numerical calculation with strength reduction method. Chin J Rock Mechan Eng S1:2749–2754

10. Jiang F, Zhang JY (2008) Study on mechanical properties between plant roots and slope soil masses. J Geol Hazards Environ Preserv 01:57–61
11. Li JX, He BH, Chen Y, Huang R, Tao J, Tian TQ (2013) Root distribution characteristics of different herbs for slope protection and their effects on soil shear strength. Trans Chin Soc Agric Eng 29(10):144–152
12. Du XM (2020) Study on slope stability under the combined action of rainfall and earthquake based on Midas-GTS. Chongqing Jiaotong University, Chongqing
13. GB 50011-2010 (2010) Code for seismic design of buildings
14. Jiang ZQ, Sun SL, Cheng LF (2005) Analysis of soil consolidation by roots and stability of plant slopes. Site Invest Sci Technol 04:12–14